Available online at www.sciencedirect.com
ScienceDirect
Journal of Nuclear Materials 367–370 (2007) 217–221
journal of nuclear materials
www.elsevier.com/locate/jnucmat

Effect of irradiation on the microstructure and the mechanical properties of oxide dispersion strengthened low activation ferritic/martensitic steel

A. Ramar, N. Baluc, R. Schäublin *

Ecole Polytechnique Fédérale de Lausanne (EPFL), Centre de Recherches en Physique des Plasmas, Association Euratom – Confédération Suisse, 5232 Villigen PSI, Switzerland

Abstract

Ferritic/martensitic (F/M) steels show good resistance to swelling and low damage accumulation upon irradiation relative to stainless steels. 0.3 wt% yttria particles were added to the F/M steel EUROFER 97 to produce oxide dispersion strengthened (ODS) steel, to increase the operating temperature as well as mechanical strength. ODS EUROFER 97 was irradiated in the PIREX facility with 590 MeV protons to 0.3, 1 and 2 dpa at 40 °C. Microstructure of the irradiated samples is analyzed in the transmission electron microscope using bright field, dark field and weak beam conditions. The presence of voids and dislocation loops is observed for the higher doses, where as at low dose (0.3 dpa) only small defects with sizes of 1–3 nm are observed as black dots. The relationship between the defect density to dispersoids is measured and the Burgers' vector of dislocation loops is analyzed.

1. Introduction

The oxide dispersion strengthening (ODS) is an efficient approach to improve the high temperature strength of the F/M steels [1,4], since operation of the base materials such as EUROFER 97 is limited to 550 °C. It is found that the addition of 0.3 wt% yttria increases the mechanical strength by 10–20% of the EUROFER 97 [2]. At high temperatures up to 700 °C the strength of the ODS steel is maintained with good ductility [3].

The effect of irradiation on ferritic/martensitic steels leads to strong hardening and reduction in elongation starting at the lowest doses [5,6]. The fracture properties are strongly degraded with a shift in the ductile to brittle transition temperature (DBTT) above room temperature [7]. However, the damage accumulation in ferritic/martensitic steel with bcc structure is less than in other metals such as stainless steel or pure fcc metals [8]. After high energy proton/neutron irradiations to low doses, transmission electron microscopy observation reveals in F/M steel F82H unidentified defects the so-called 'black dot' [7,8] possibly interstitial clusters, with sizes ranging from 1 to 2 nm [9,10]. In another ferritic/martensitic steel, Optimax, the irradiation induced hardening reduces the total

* Corresponding author. Tel.: +41 56 310 40 82.
E-mail address: robin.schaeublin@psi.ch (R. Schäublin).

0022-3115/$ - see front matter © 2007 Elsevier B.V. All rights reserved.
doi:10.1016/j.jnucmat.2007.03.142

elongation and shifts the DBTT value to higher temperatures, which is due to the formation of nanocavities and small sized defect clusters [14]. Irradiation induces hardening is also observed in oxide dispersion strengthened steel [12,13].

The investigated materials were irradiated at room temperature. The attempt has been made to explain irradiation induced hardening based on a relationship between the number density of the dispersed yttria to irradiation induced defects in the matrix of ODS EUROFER 97. The objective of the present work is to provide information about the effects of irradiation on the mechanical and microstructural changes of the ferritic ODS EUROFER 97 from Plansee.

2. Experimental

ODS EUROFER 97 was irradiated in the PIREX (proton irradiation experiment) facility with 590 MeV protons to doses of 0.3, 1 and 2 dpa at 40 °C, at the Paul Scherrer Institute. Microhardness tests were performed on the specimens at different irradiation doses and the obtained results were related to the strength of the unirradiated material. TEM specimens prepared with special technique [9] were investigated in a JEOL2010 electron microscope with LaB_6 gun, high tilt lens, operated at 200 kV. The microstructure of the irradiated samples was analyzed using the bright field, dark field and weak beam conditions. Nanobeam diffraction method was used to identify any phase transitions in the yttria particles such as amorphization.

Table 1
Vickers microhardness of unirradiated and irradiated ODS EUROFER 97, with defect density present for different irradiated dose

Irradiated condition (dpa)	Vickers microhardness	Defect number density (10^{22} m^{-3})	$\Delta\sigma$ (MPa) (Calculated)
Unirradiated	338	None	None
0.3	338	2.3	11.17
1	351	4.4	19.24
2	389	5.1	43.69

3. Results and Discussion

The material irradiated to 0.3 dpa and 1 dpa shows measured hardening of about 3%. At 2 dpa, the material shows significant hardening of about 10–15% (Table 1) as observed by uniaxial tensile test of the material [13]. The microstructure of the ODS ferritic/martensitic steel after irradiation shows an unaltered homogeneous ferrite structure with rather equiaxed grains and a low dislocation density.

Fig. 1 shows a 0.3 dpa irradiated ODS sample imaged by dark field weak beam with **g**(5**g**) condition using $\mathbf{g} = \{0\,1\,1\}$. Upon irradiation, the microstructure of the material shows few small black dots with sizes ranging from 1 to 2 nm (Fig. 2(A)). The density of the defects and the dispersed yttria particle were measured and found to be about 2.3×10^{22} m^{-3} and 4.5×10^{22} m^{-3}, respectively.

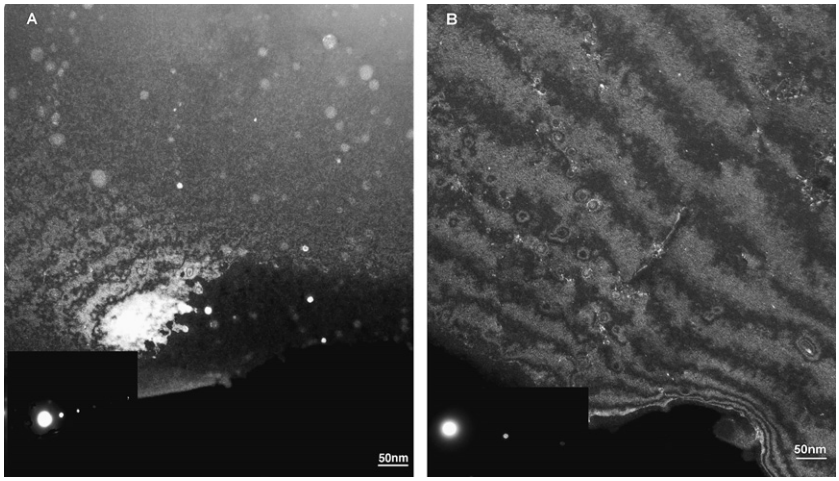

Fig. 1. TEM weak beam image with **g**(5**g**) condition with $\mathbf{g} = \{0\,1\,1\}$ close to $\{1\,1\,1\}$ zone axis of ODS EUROFER 97 irradiated to 0.3 dpa showing yttria particles as light grey dots and small defects like white dots (A) and clearly visible irradiation induced defects as small white dots (B).

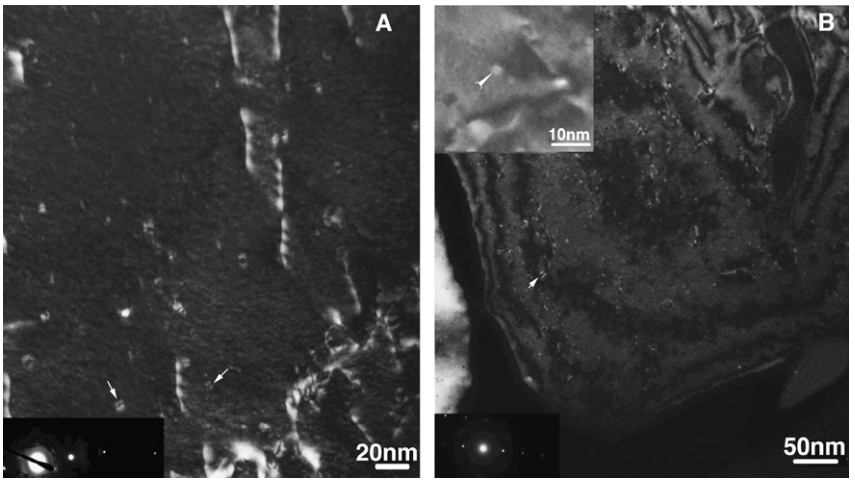

Fig. 2. TEM weak beam image using $\mathbf{g}(5\mathbf{g})$ $\mathbf{g} = \{1\,1\,2\}$ close to $\{1\,1\,1\}$ zone axis of ODS EUROFER 97 irradiated to 1 dpa showing (A) dislocation lines and clearly visible loops and (B) clearly visible irradiation induced defects as small white dots using $\mathbf{g}(4\mathbf{g})$ $\mathbf{g} = \{1\,1\,0\}$ close to $\{0\,0\,1\}$ zone axis small dots appear to be loops at higher magnification as shown by arrow (B inset).

The mean size of the dispersed yttria particles is about 6–10 nm. The density of the yttria particles deduced from the mean particle size is $4.5 \times 10^{22}\ \mathrm{m}^{-3}$ for the total volume of the ball milled powder. It is observed that the density of the irradiation induced defects is less than the yttria particles, which explains the low hardening.

Fig. 2 shows the dark field weak beam images using $\mathbf{g}(5\mathbf{g})$, $\mathbf{g} = \{1\,1\,0\}$ (Fig. 2(A)) and $\mathbf{g} = \{1\,1\,2\}$ (Fig. 2(B)) of the microstructure of the ODS sample irradiated to 1 dpa. The microstructure of the material comprises dislocation loops and some black dots (Fig. 2(A)). The black dots observed at higher magnification present contrast features typical of dislocation loops with sizes ranging from 2 to 3 nm (Fig. 2(B) inset). The density of the defects and the dispersed yttria particles were measured and found to be about $4.1 \times 10^{22}\ \mathrm{m}^{-3}$ and $4.5 \times 10^{22}\ \mathrm{m}^{-3}$, respectively. At this low dose, the material shows a defect density equal to the dispersed particles, which explains the very low hardening in the material, since the obstacle strength of yttria is higher than that of the irradiation induced defects.

Fig. 3 shows the bright field (Fig. 3(A)) and dark field weak beam images using $\mathbf{g}(4\mathbf{g})$, $\mathbf{g} = \{1\,1\,0\}$

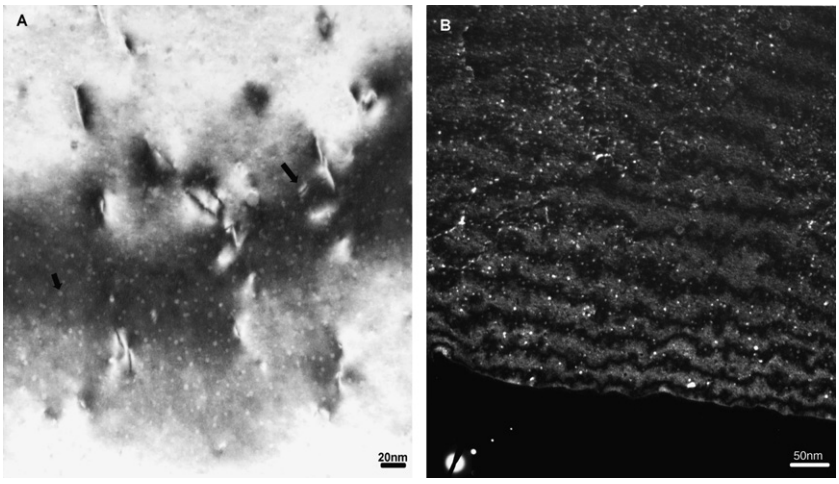

Fig. 3. TEM bright field image of ODS EUROFER 97 irradiated to 2 dpa showing (A) clearly visible nanocavities and dislocation loops and (B) irradiation induced defects as small white dots using $\mathbf{g}(4\mathbf{g})$, $\mathbf{g} = \{1\,1\,0\}$ close to $\{1\,1\,1\}$ zone axis.

(Fig. 3(B)) of the ODS sample irradiated to 2 dpa. The microstructure of the material comprises nano cavities and dislocation loops in the bright field condition (Fig. 3(A)). In the dark field weak beam condition with $\mathbf{g} = \{1\,1\,0\}$ at $\mathbf{g}(4\mathbf{g})$ condition, dislocation loops with sizes 5–10 nm and a high density of black dots are observed. The nanocavities are found higher in number density with the size range of 2–5 nm in the bright field condition (Fig. 3(A)). The density of the defects and the dispersoid were measured and found to be $5.1 \times 10^{22}\ m^{-3}$ and $4.5 \times 10^{22}\ m^{-3}$, respectively. At the highest dose (2 dpa) in this study the irradiation induced defect density is higher than the dispersed yttria particle density, which explains the significant hardening in the material.

The **g**.**b** analysis was done to determine the Burgers vector of the dislocation loops as shown in Fig. 4. Most of the loops are visible with $\mathbf{g} = \{2\,0\,0\}$ and half of them are visible with $\mathbf{g} = \{1\,1\,0\}$, when the sample normal is $\{1\,1\,0\}$ and $\{1\,1\,1\}$, respectively. It is deduced from this observation that the loops have a Burgers vector $\mathbf{b} = 1/2a_0\ \langle 1\,1\,1\rangle$, for all of them are visible with $\mathbf{g} = \{2\,0\,0\}$ and half of them are visible with $\mathbf{g} = \{0\,1\,1\}$ [9–11].

Fig. 5 shows a yttria particle in the ODS EUROFER97 irradiated to 1 dpa at room temperature. Nanobeam diffraction was performed on the central yttria particle with a nominal beam size of 7 nm. The diffraction pattern on the particle (inset in Fig. 5) shows a ring, which indicates amorphization.

The dispersed barrier hardening model expresses hardening due to a dispersion of obstacles as a function of their density and size with the following relationship, $\Delta\sigma = M\alpha\mu b(Nd)^{1/2}$, where M is the Taylor factor, α is the obstacle strength, μ the shear modulus, b the burgers vector, N the defect density and d the defect mean size. The values used to calculate the hardening in the EUROFER 97 matrix are as follows, M – 0.3, $\mu = 78.974$ GPa, $b = 0.286$ nm, the obstacle strength (α) was taken as 0.3 and 1 for irradiation induced defects and dispersed yttria particles, respectively. The hardening caused by the mean size of the dispersed yttria particles is 141.72 MPa and the hardening calculated with the defect density of irradiation induced defect is given in Table 1 for EUROFER 97 matrix. The increase

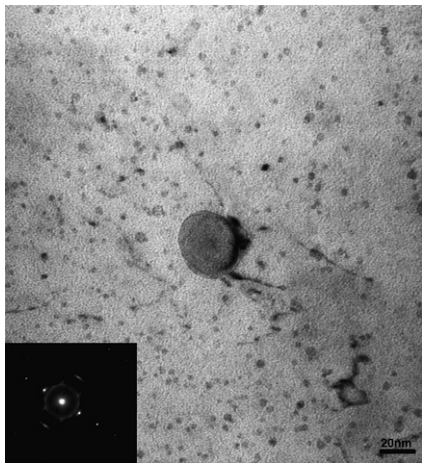

Fig. 5. ODS EUROFER97 irradiated to 1 dpa at room temperature. Nanobeam diffraction pattern (inset) performed on the central yttria particle in the picture shows a ring, which indicates amorphization.

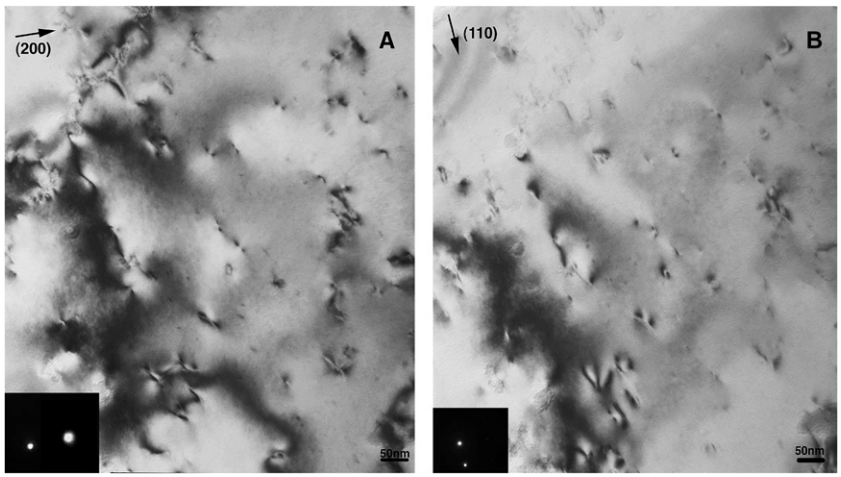

Fig. 4. TEM bright field image of ODS EUROFER 97 irradiated to 1 dpa imaged with (A) $\mathbf{g} = \{2\,0\,0\}$ and (B) $\mathbf{g} = \{0\,1\,1\}$ showing dislocation loops.

in Vickers hardness in the irradiated material with different doses follows the calculated hardening values, except for 0.3 dpa. It can be observed that the material irradiated to 0.3 dpa and 1 dpa presents low hardening value compared to hardening by the dispersed yttria particle. At a dose of 2 dpa, the hardening by the defect is close to one third of the hardening by the dispersed yttria particle, which explains the significant hardening in the material.

4. Conclusions

Irradiation of ODS EUROFER97 from Plansee produces the following effects:

(1) Small black dots of the size 1–2 nm at 0.3 dpa, whereas dislocation loops, nanocavities with size 3–5 nm and small black dots are observed at doses of 1 and 2 dpa.
(2) Loops have a Burgers vector of $\mathbf{b} = 1/2a_0\langle 1\,1\,1\rangle$.
(3) Some of the dispersed yttria particles with sizes from 10 to 20 nm are amorphized.
(4) At a dose of 2 dpa, irradiation induced defects are higher in number density than the dispersed yttria particles, which although they are weaker than the yttria particles can explain the significant hardening observed in the material.

Acknowledgements

The Paul Scherrer Institute is acknowledged for the overall use of the facilities. EFDA is acknowledged for financial support.

References

[1] R.L. Klueh, D.J. Alexander, J. Nucl. Mater. 223–237 (1996) 336.
[2] A. Hishinuma, A. Kohyama, R. Klueh, D.S. Gelles, W. Dietz, K. Ehrlich, J. Nucl. Mater. 253–258 (1998) 193.
[3] E. Lucon, Fus. Eng. Des. 61&62 (2002) 683.
[4] R. Schäublin, T. Leguey, P. Spätig, N. Baluc, M. Victoria, J. Nucl. Mater. 307–311 (2002) 778.
[5] D.K. Mukhopadhyay, F.H. Froes, D.S. Gelles, J. Nucl. Mater. 258–263 B (1998) 1209.
[6] P. Spätig, R. Schäublin, S. Gyger, M. Victoria, J. Nucl. Mater. 258–263 (1998) 1345.
[7] J. Rensman, H.E. Hofmans, E.W. Schuring, J. van Hoepen, J.B.M. Bakker, R. den Boef, F.P. van den Broek, E.D.L. van Essen, J. Nucl. Mater. 307–311 (2002) 250.
[8] M. Victoria, N. Baluc, C. Bailat, Y. Dai, M.I. Luppo, R. Schäublin, B.N. Singh, J. Nucl. Mater. 276 (1–3) (2000) 114.
[9] R. Schäublin, D. Gelles, M. Victoria, J. Nucl. Mater. 307–311 (2002) 197.
[10] R. Schäublin, M. Victoria, J. Nucl. Mater. 283–287 (2000) 339.
[11] D.S. Gelles, J. Nucl. Mater. 239 (1996) 99.
[12] R. Schäublin, M. Victoria, in: G.E. Lucas, L. Snead, M.A. KirkJr, R.G. Elliman (Eds.), Microstructural Processes in Irradiated Materials, Mat. Res. Soc. Symp. Proc. 650 (2001) R1.8.1.
[13] R. Schäublin, A. Ramar, N. Baluc, V. de Castro, M.A. Longe, T. Leguey, N. Schmid, C. Bonjour, J. Nucl. Mater. 251 (2006) 247.
[14] N. Baluc, R. Schäublin, C. Bailat, F. Paschoud, M. Victoria, J. Nucl. Mater. 283–287 (2000) 731.